Reprinted from Preprint Volume: Nineteenth Conference on Radar Meteorology, April 15-18, 1980, Miami, Fla.
Published by the American Meteorological Society, Boston, Mass.

3.1

DOWNBURSTS AND MICROBURSTS
--AN AVIATION HAZARD--

T. Theodore Fujita

The University of Chicago
Chicago, Illinois

1. INTRODUCTION

The term, "Downburst", introduced by Fujita (1976) and Fujita and Byers (1977), was defined as being a downdraft which induces damaging winds on or near the ground. Subsequent research on aircraft accidents by Fujita and Caracena (1977) and aerial photographic mapping of downburst damages by Fujita (1978) revealed a wide range of the horizontal dimensions:- several tenths to several tens of miles, a difference of two orders of magnitude.

In order to distinguish large downbursts from small ones, Fujita (1978,1979) called mini-size downburst, the "Microburst". The division between downbursts and microbursts was chosen to be $\sqrt{10}$ = 3.16 miles or 5 km in horizontal dimensions.

It is the microburst which induces dangerous winds during the takeoff and landing stages of jet aircraft. By virtue of its small horizontal scale, a microburst could induce a strong headwind-to-tailwind shear in addition to a significant downflow extending near the ground.

Table 1 shows seven documented cases of microburst-related aircraft accidents and incidents which resulted in a total of 144 deaths and 140 injuries. None of these local winds were predicted or detected in time for warning the pilots of extreme wind shear they were going to fly through.

It is suspected that there had been many other incidents which were not reported because pilots could control the aircraft for successful fly out.

Table 1. Microburst-related incidents known to the author as of November 1979. Causes of a number of other incidents, such as the fatal accident at Doha Airport, Qatar, at 3:30 am on March 14, 1979, are likely to be similar in nature, but they have not been documented yet. Hw and Tw denote head and tailwinds, respectively.

Year	1956	1975	1975	1975	1976	1977	1979
Date Standard time	June 24 5:23 pm	June 24 2:57 pm	June 24 3:05 pm	August 7 4:11 pm	June 23 4:12 pm	June 3 12:59 pm	August 22 2:12 pm
Airport Flight During	Kano BOAC 252 Takeoff	JFK EA 902 Landing	JFK EA 66 Landing	Denver CO 426 Takeoff	Philadelphia AL 121 Landing	Tucson CO 63 Takeoff	Atlanta EA 693 Landing
Fatalities Injured	32 7	go around	112 12	Zero 15	Zero 106	returned	go around
Microburst Diameter	3.5 km 2.2 mi	4.8 km 3.0 mi	4.1 km 2.5 mi	5.0 km 3.1 mi	2.8 km 1.8 mi	3.1 km 1.9 mi	2.5 km 1.5 mi
Headwind Shear	20 kt Hw to strong Tw	11 kt Hw to 4 kt Tw	16 kt Hw to 4 kt Hw	10 kt Hw to 50 kt Tw	65 kt Hw to calm	30 kt Hw to 30 kt Tw	2 kt Hw to 55 kt Hw
Downflow at AGL Height	----- -----	20 fps 200 ft	25 fps 250 ft	3 fps 70 ft	15 fps 260 ft	3 to 5 fps 100 ft	60 fps 700 ft

2. FOUR STAGES OF MICROBURST

Numerous aerial photographs of microburst damages taken in the Midwest show that wind effects suddenly appear on the ground and disappear completely within one to three miles.

Evidence has led to a suspicion that a microburst is a short-lived, transient phenomenon. In spite of such a suspicion, no proof of a microburst in action was available until July 1, 1978, when Mike Smith, a TV weatherman at Wichita, Kansas, took a sequence of pictures.

The sequence of pictures in Figure 1 reveals the formation and development of a microburst which descended from the cloud base at about 1.5 km (5,000 ft). The diameter of the downburst core was 1.0 to 1.2 kms (3 to 4,000 ft).

Four stages of the evolution of a microburst, as implied by Smith's pictures and wind effects of other microbursts are :

A. DESCENDING STAGE

An air current descends with precipitation that evaporates inside the downflow. The precipitation looks

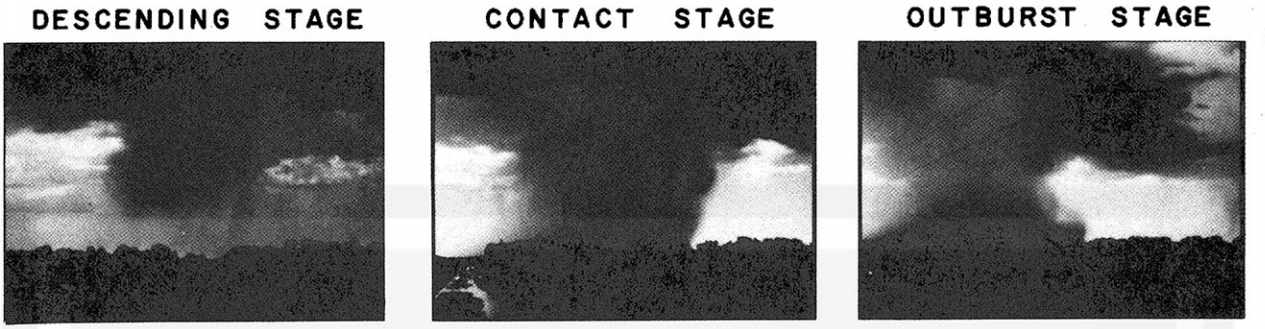

Figure 1. Microburst in action, July 1, 1978. Copyrighted pictures by Mike Smith.

innocent enough and a flight beneath the descending virga is expected to be smooth.

B. CONTACT STAGE

The downflow hits the ground. Precipitation may or may not reach the ground, depending upon the drop-size distribution, height of the cloud base, environmental relative humidity, etc..

C. OUTBURST STAGE

The outflow spreads out violently within the 100- to 200-m (300 to 500 ft) layer above the ground. An arc of the outburst front pushes outward from the downburst center.

D. DISSIPATING STAGE

Within a few minutes the source of the downflow is exhausted, while the outburst front keeps expanding with a curl-back motion of the outburst air. A giant smoke ring expands while growing in size and weakening in intensity very rapidly.

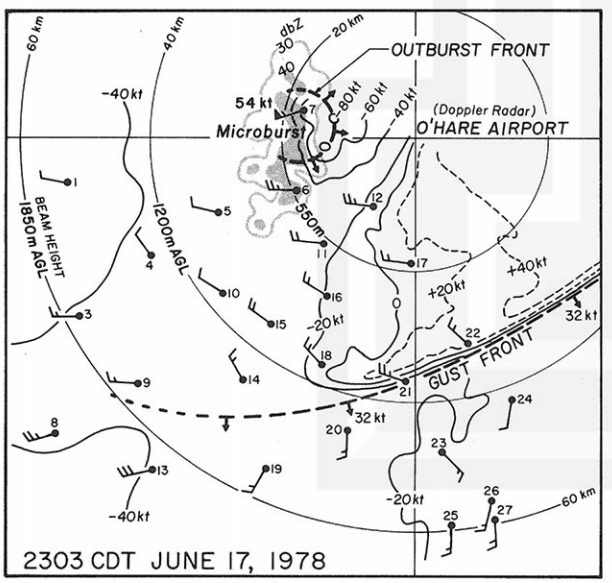

Figure 2. A gust front and a microburst over the Project NIMROD network.

3. GUST FRONT AND MICROBURST

It is unfortunate that the so-called gust front, which had been documented by Faust (1947), Newton (1950), Goff (1976) and many others, has been mixed up in various occasions with microburst, in terms of their meteorological definitions and their effects upon penetrating aircraft.

Some meteorologists argue controversially that a microburst could be a perturbation on or near a gust front. Project NIMROD (Northern Illinois Meteorological Research on Downburst) network was operated in Summer 1978 to clarify the nature of the controversy.

Analyses of the NIMROD data began showing convincingly the difference between the gust front and the downburst. Figure 2, for example, shows the pattern of Doppler velocities by a Doppler radar (NCAR CP-4) at O'Hare airport. Two other Doppler radars were located at Yorkville (NCAR CP-3) and at Monee (CHILL).

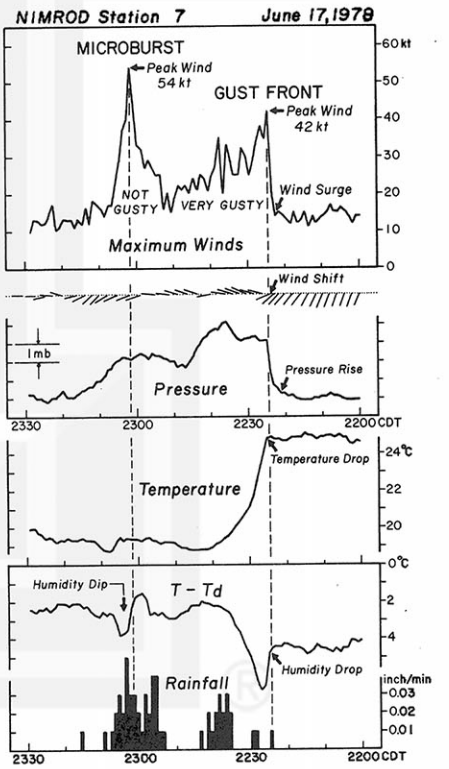

Figure 3. Records of meteorological parameters from PAM Station No. 7, 11 miles west-northwest of O'Hare Airport.

A. GUST FRONT (CLASSICAL)

A gust front is a front of a sudden and brief increase of wind followed by a succession of peak and lull in windspeeds. The flow is predominantly horizontal, characterized by large gustiness factors.

A gust front travels tens of miles out from thunderstorm areas accompanied by temperature drop and pressure rise. Relative humidity either rises or drops depending upon precipitation and turbulent mixing behind the front.

The life of a gust front is 30 minutes to several hours, permitting researchers to apply steady-state assumptions while dealing with an overall gust front.

B. MICROBURST

A microburst is a peaked increase and decrease of wind with small gustiness. The flow is both horizontal (highly divergent) and downward. Divergence near the ground may reach 0.5 per second with downward current of 5 m/sec (15 fps) at 10 m (30 ft) AGL.

Radar reflectivity in and around a strong microburst could be lower than its environment due to a rapid evaporation in the descending currents.

A microburst may occur either on the front side or on the back side of a gust front or without a gust front nearby. Since a microburst is very short-lived, one to five minutes, it cannot be assumed to be a steady-state wind system at the source, contact, and outburst regions.

The classical gust front, depicted by the Doppler velocity field and surface winds from the PAM network, extends several tens of kilometers across the NIMROD network. The trace of the maximum winds at one-minute intervals at PAM station No. 7 (see Figure 3) shows the passage of the gust front followed by very gusty winds.

A microburst, on the other hand, is characterized by a rapid surge and fall of windspeeds which are relatively gust-free. The air newly descended to the ground may not have time to induce significant turbulent eddies contributing to gustiness.

4. ATLANTA AIRPORT INCIDENT

During the past few years, networks of anemometers were established at major airports across the United States. The system, called the Low Level Wind Shear Alert System (LLWSAS), is designed to initiate a wind shear alarm if preset thresholds are exceeded by 15 kt vector difference, 9 kt gust factor, for example.

Figure 4 shows the distribution of six anemometers in relation to three runways at Atlanta Airport. If a classical gust front approaches from the north or northwest, the LLWSAS will pick up the preset thresholds to activate an alarm.

Figure 4. Location of six LLWSAS anemometers at Atlanta Airport.

On August 22, 1979, however, a B-727 aircraft on the 27-L glidepath encountered a serious difficulty, resulting in a successful go-around. Two documents by the NTSB on this Atlanta Airport incident are:

A. Factual Performance Report of Investigation by Macidull dated September 28, 1979

B. Weather Condition Investigation by Salottolo, Coons, Biggers, and Cornay dated October 1, 1979.

The author made a preliminary attempt to determine if the incident could be explained by the existence of a microburst on the glidepath or not. The result presented in this paper does not exclude other possibilities such as proposed by Frost et al. (1978) and McCarthy et al. (1978).

4.1 RADAR OVERVIEW

The National Weather Service's WSR-57 radar at Athens, Ga, was used to determine the specific radar echo which was located on or near the Atlanta Airport at the time of the incident at 1912 GMT.

The storm's first echo appeared on the radar scope at 1802 (see Figure 5). The echo was one of those air-mass showers scattered all around the airport. At 1845, 43 min. after the first echo, NWS anemometer at the airport (see Figure 4 for the location) recorded a 32 kt peak gust from the northwest.

Thereafter, the echo decreased in size and dissipated at 1918, after its total life of 1 hr 16 min. It should be noted that the incident occurred at 1912, 6 min before the echo on the Athens radar dissipated.

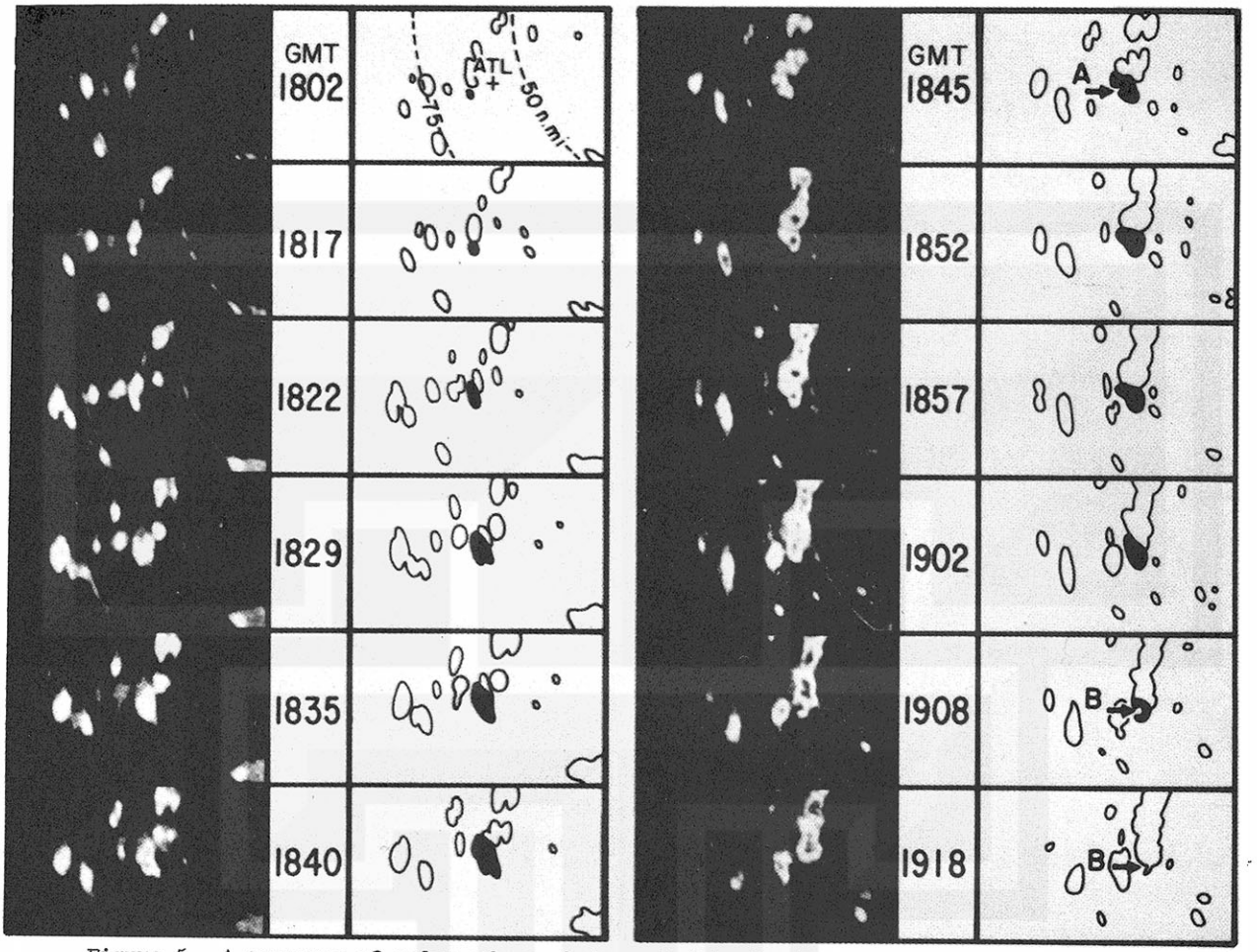

Figure 5. A sequence of radar echoes photographed by the NWS Athens radar between 1802 and 1918 GMT on August 22, 1979. The echo which caused a 32-kt gust and the microburst on the 27-L approach were painted.

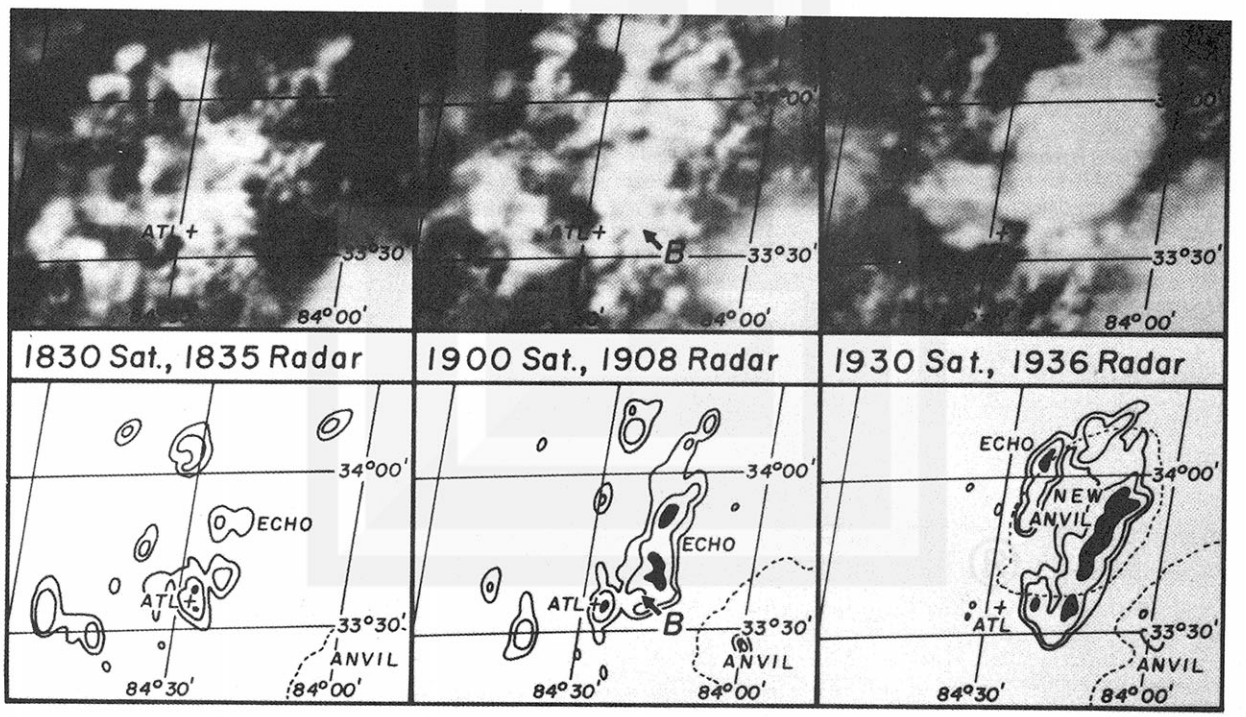

Figure 6. Three SMS pictures on August 22, 1979. Enlargement of 9" x 9" negatives from Linwood Whitney of NESS. Radar echoes are from NWS Athens.

4.2 SATELLITE OVERVIEW

Air mass showers prevailed over the southern United States for several days around August 22, when the incident occurred. On August 21, a sequence of rapid-scan SMS pictures taken at 3 min intervals, was requested by Fujita, thus missing by one day to document the Atlanta situation.

Linwood Whitney of NESS obtained for the author SMS pictures on August 22, taken for every 30 minutes. These were the only pictures available on that day, but their quality, recorded on 9" x 9" negatives, is excellent.

Three pictures from the sequence were enlarged and gridded with latitudes and longitudes for every $\frac{1}{2}$ degree (see Figure 6).

Radar echoes from Athens were distorted to fit the perspective of the SMS pictures. Note that the time of SMS pictures is the picture-start time while the radar time is chosen to be close to the scan time over the Atlanta area.

The closest pictures to the time of the aircraft incident are 1900 satellite and 1908 radar pictures. An arrow with B denotes the location where the aircraft encountered the difficulty.

4.3 AIRCRAFT DATA

Flight recorder analysis by Macidull (1979) was used as the sole data source to estimate both headwind and downwind shear.

The curve of W_a in Figure 7 was obtained by integrating the vertical acceleration with respect to time.

$$W_a = \int_0^t a\,dt + W_o \qquad (4.1)$$

where "a" denotes the vertical acceleration in "G" units; W_a, the vertical velocity (rate of descent) of the aircraft; and W_o, the vertical velocity at the initial time of the integration. One-second time steps were used for computing W_a.

W_p, the vertical velocity (rate of descent) was also computed independently by differentiating the pressure altitude with time. Then the curve of W_p was superimposed upon that of W_a to determine

$$W_o = -12 \text{ fps}. \qquad (4.2)$$

The vertical velocity of the aircraft, W and that of the air, w are different, because an aircraft has its own climb or descent capability relative to its environmental airflow.

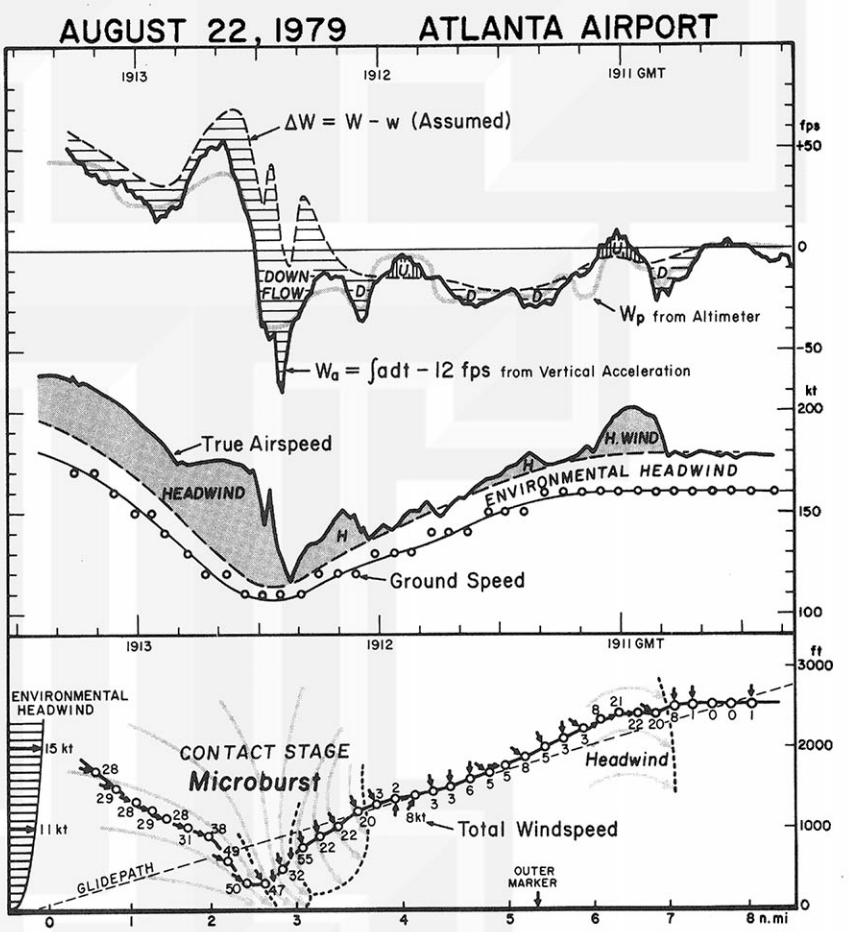

Figure 7. Flight path, headwind and vertical velocity of EA693. Based on Macidull (1979)

Macidull (1979) points out that $\Delta W = W - w$, the climb capability depends on such factors as (1) pitch angle, (2) power application, (3) airspeed, (4) gross weight, (5) density altitude, and (6) aircraft configuration. Unfortunately, (1), (2), and (6) were not available on any recorded data. On page 5 of the Macidull report, the downdraft at 1912 + 19 sec GMT was estimated to be between 49 fps and 68 fps.

The author made an initial attempt to assume ΔW, the climb capability during the descent period, to estimate further the vertical motion of the air from

$$w = W - \Delta W. \qquad (4.3)$$

The middle diagram in Figure 7 is the true airspeed and the radar groundspeed from Macidull. The shaded area, representing the headwind, was obtained by the author by subtracting the environmental headwinds to be encountered by any aircraft descending through a weak, natural shear environment.

The shaded downwinds and downflow speeds, w, were combined vectorially in the lower diagram in Figure 7 to obtain the airflow of a microburst in its contact stage.

Figure 8 reveals the downflow and headwinds encountered by the incident aircraft during its final approach inside the outer marker. It should be noted that Macidull's calculations show that there were little or no cross winds during the approach and go-around.

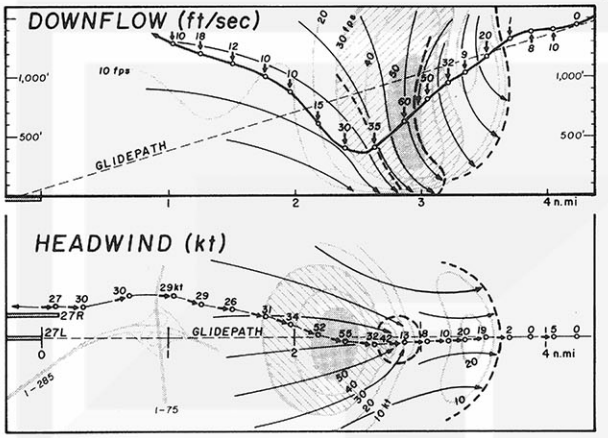

Figure 8. Estimated downflow and headwind encountered by EA 693 at Atlanta.

4.4 RADAR ECHOES

The painted radar echo in Figure 5 moved directly over the Airport area from west to east. At the begining the traveling speed was about 12 kt. It, then, slowed down.

At 1840 GMT the echo was centered over the Airport (Figure 9). Time-space conversions of rain and thunder observed at the NWS Forecast Office (NWSFO) and transmissivity (visibility) traces from Salottolo et al. (1979) fit very well with the extent of the echo.

A weak echo hole "A" was located to the south of the NWS anemometer when it measured a peak gust of 32 kt at 1845. Ea 693 incident occurred at 1912 GMT, some 27 min later. For anemometer trace and echo, refer to Figure 10.

In a few minutes the hole "A" was gone while the center of a strong reflectivity inside the echo began moving eastward along the glidepath of 27-L (Refer to Figures 11,12, and 13).

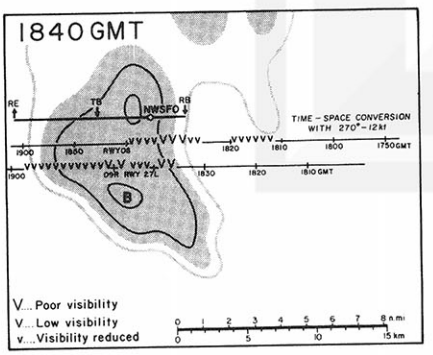

Figure 9. Echo at 1840 GMT

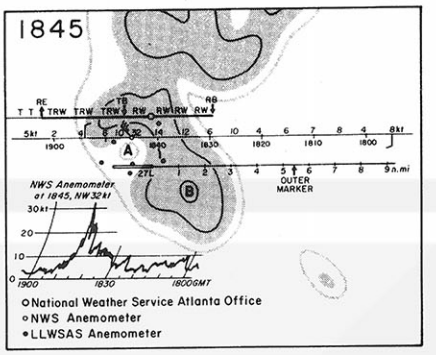

Figure 10. Echo at 1845 GMT

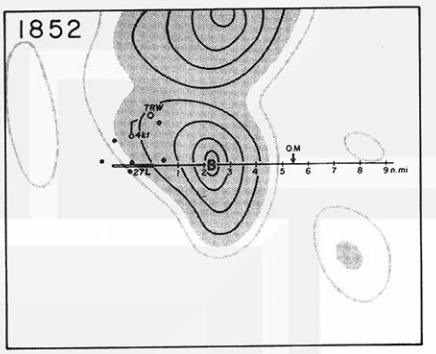

Figure 11. Echo at 1852 GMT

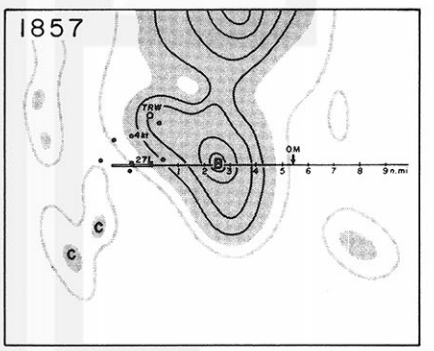

Figure 12. Echo at 1857 GMT

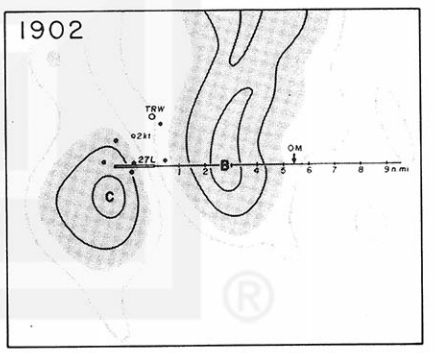

Figure 13. Echo at 1902 GMT

Then suddenly, the high reflectivity center turned into a hole "B" in Figure 14. It was four minutes later when EA 693 encountered a difficulty.

In ten minutes the weak-echo hole disintegrated and the echo was gone. This analysis of the radar echo shows that the incident occurred inside the area of the weak-echo hole shortly before the echo disappeared from the Athens radar scope.

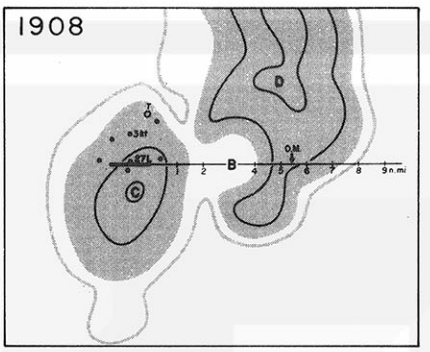

Figure 14. Echo at 1908 GMT

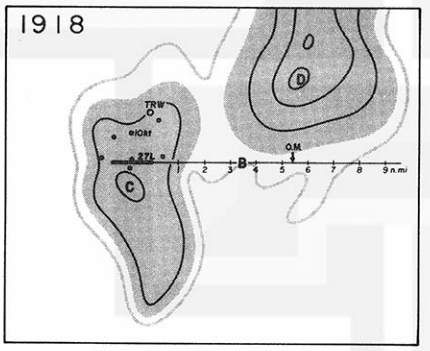

Figure 15. Echo at 1918 GMT

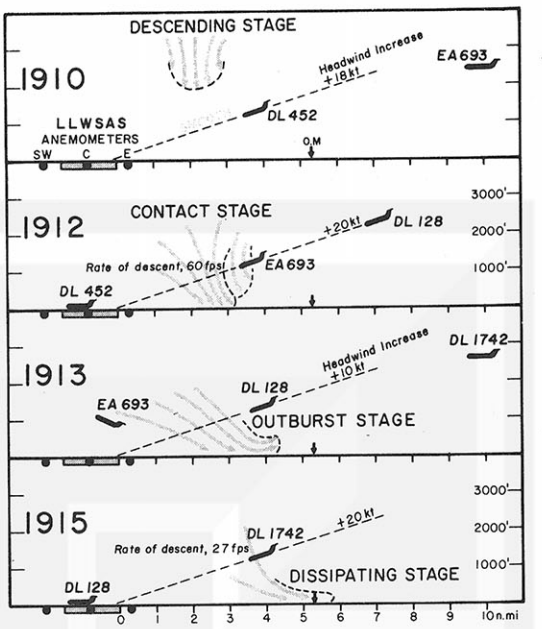

Figure 16. Four aircraft on the 27-L approach path on August 22, 1979. Due to its small size and the short life, a microburst does not affect approaching aircraft uniformly. It is unlikely that any anemometer network inside an airport is able to depict the microburst winds on the approach path.

DL 1742 experienced its greatest rate of descent of over 27 fps (1600 fpm) for 11 seconds where EA 693 encountered the difficulty. The pilot, after landing, transmitted to the tower ".. ...you got a nice shear out there inside the marker".

4.5 OTHER AIRCRAFT ON THE APPROACH

Macidull's report identified three other aircraft on the 27-L approach. They were DL 452 which descended two minutes earlier and DL 128 and DL 1742 which followed EA 693, one to three minutes later.

A summary of the events experienced by these aircraft is shown in Figure 16 along with aircraft positions and the estimated stages of the microburst on the glidepath.

Macidull's report revealed that all aircraft experienced an increase in the headwind outside the outer marker. The increase, 10 to 20 kt occurred to the east of the echo boundary which crossed the glidepath near the outer marker.

DL 452 approached slightly fast (160 kt) with smooth descent all-the-way to touchdown.

EA 693 experienced a difficulty leading to the go-around, reaching the minimum altitude of 400 ft AGL.

DL 128 maintained approximately 15 fps (900 fpm) rate of descent to touchdown.

5. MICROBURST:--AN INDUCER OF STRONG HORIZONTAL & DOWNWARD WINDS ON THE GROUND

Numerous photographic evidence of microburst winds on the ground has been obtained through extensive aerial photographic surveys.

The maximum horizontal outburst winds could reach as high as 150 mph. Tree damage in Figure 17, for example, is worse than that which existed near the Dauphin Is. bridge where 130 mph winds were recorded during Hurricane Frederic.

Vertical wind near the ground should not be underestimated. A high-wind streak in the corn field in Figure 18 was caused by a wind of 70 mph (60 kt). If the descending angle is between 20 and 30 degrees, the vertical current at the roof top will be 20 to 35 kt (35 to 60 fps).

Six cases of aircraft accidents/incidents in Table 1 were plotted on a headwind vs downflow diagram. The distribution of the incident dots suggest strongly that the domain of DANGER is on the lower left side of the diagram where the combined effects of the headwind decrease and the downflow intensity are significant.

Figure 17. Tree damages caused by a microburst of August 10, 1979 in Michigan. Estimated windspeed, 150 mph. Photo by Wakimoto.

Figure 18. Downburst winds deflected by a slanted roof. September 30, 1977 storm in Indiana. Estimated downward current on the roof, 35 to 60 fps. Photo by Fujita.

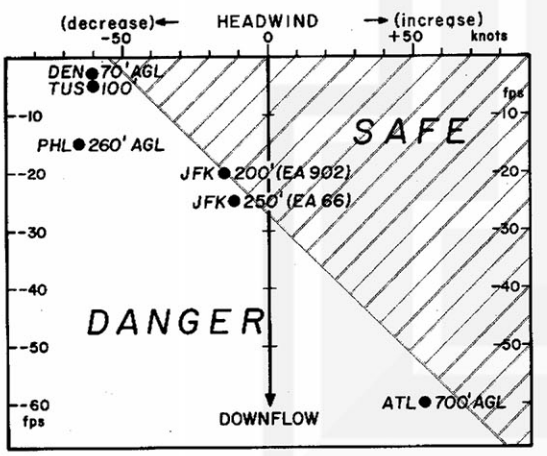

Figure 19. The domain of danger evidenced by the six flights through microbursts in Table 1.

6. CONCLUSIONS

The author's research on downburst/microburst phenomena since 1975 has led to a number of conclusions listed below. The conclusions are the reflection of his personal views supported by his meteorological analyses of aircraft accidents/incidents, aerial surveys of wind effects left behind downbursts, and other evidence in support of the existence of sub-mesoscale (miso-scale) wind systems.

(1) Microbursts beneath small, air mass thunderstorms are unpredictable in terms of weather forecast.

(2) Most aircraft accidents/incidents have been occurring in summer months, June through August.

(3) An intense microburst could produce 150 mph horizontal winds as well as 60 fps downflows at the tree-top level.

(4) A combination of the headwind decrease and the downflow appears to be the largest contributing factor causing difficulties.

(5) Anemometers and/or pressure sensors placed near runways are effective for detecting classical gust fronts, but not for downbursts.

(6) New detection system, either on the ground or airborne, must be developed quickly.

(7) It is recommended that pilots be trained for simulated landing and go-around through microbursts.

The author does not think personally that the current systems are 100% effective for the prevention of another aircraft accident in a microburst.

We should learn more about the nature of microbursts in relation to GOES/SMS pictures, radar signatures, and surface data.

Acknowledgement:- Research supported by NESS, Grant No. 04-4-158-1; NASA, Grant No. NGR 14-001-008; and the Atmospheric Research Section, National Science Foundation, Grant No. ATM 78-01074.

REFERENCES

Faust, H. (1947): Untersuchungen von Forstschäden hinsichtlich der windstructetur bei einer Bö. Meteor. Rundschau, 1, 290-297.

Frost, W. and B. Crosby (1978): Investigation of simulated aircraft flight through thunderstorm outflow. Report to Marshall Space Flight Center by FWG Associates, Inc., Tullahoma, Tennessee.

Fujita, T. T. (1976): Spearhead echo and downburst near the approach end of a John F. Kennedy Airport runway. SMRP Res. Paper 137, Univ. of Chicago, 51 pp.

Fujita, T. T. and H. R. Byers (1977): Spearhead echo and downburst in the crash of an airliner. Mon. Wea. Rev., 105, 129-146.

Fujita, T. T. and F. Caracena (1977): An analysis of three weather-related aircraft accidents. Bull. Amer. Meteor. Soc., 58, 1164-1181.

Fujita, T. T. (1978): Manual of downburst identification for Project NIMROD. SMRP Res. Paper 156, Univ. of Chicago, 104 pp.

Fujita, T. T. (1979): Objectives, operations and results of Project NIMROD. Preprint of 11th Conference on Severe Local Storms, Amer. Meteor. Soc., 259-266.

Goff, R. C. (1976): Vertical structure of thunderstorm outflows. Mon. Wea. Rev., 104, 1429-1440.

Macidull, J. C. (1979): Factual performance report of investigation. NTSB, 5 pp and 5 figures.

McCarthy, J., E. F. Blick, and R. R. Bensch (1978): A spectral analysis of thunderstorm turbulence and jet transport landing performance. Conference on Atmospheric Environment of Aerospace Systems and Applied Meteorology, Amer. Meteor. Soc., 75-82.

Newton, C. W. (1950): Structure and mechanism of the pre-frontal squall line. J. Meteor., 7, 210-222.

Salottolo, G. D., F. Coons, W. R. Biggers, and R. Cornay (1979): Weather condition investigation. NTSB, 7 pp.